HHS Public Access

NAD hydrolysis by the tuberculosis necrotizing toxin induces lethal oxidative stress in macrophages

David Pajuelo, **Norberto Gonzalez-Juarbe**[$], **Michael Niederweis**[*]

Department of Microbiology, University of Alabama at Birmingham, Birmingham, AL, USA

Abstract

Mycobacterium tuberculosis (Mtb) kills infected macrophages through necroptosis, a programmed cell death that enhances mycobacterial replication and dissemination. The tuberculosis necrotizing toxin (TNT) is the major cytotoxicity factor of Mtb in macrophages and induces necroptosis by NAD^+ hydrolysis. Here, we show that the catalytic activity of TNT triggers the production of reactive oxygen species (ROS) in Mtb-infected macrophages causing cell death and promoting mycobacterial replication. TNT induces ROS formation both by activating necroptosis and by a necroptosis-independent mechanism. Most of the detected ROS originate in mitochondria as a consequence of opening the mitochondrial permeability transition pore. However, a significant part of ROS is produced by mechanisms independent of TNT and necroptosis. Expressing only the *tnt* gene in Jurkat T-cells also induces lethal ROS formation indicating that these molecular mechanisms are not restricted to macrophages. Both the antioxidant N-acetyl-cysteine and replenishment of NAD^+ by providing nicotinamide reduce ROS levels in Mtb-infected macrophages, protect them from cell death and restrict mycobacterial replication. Our results indicate that a host-directed therapy combining replenishment of NAD^+ with inhibition of necroptosis and/or antioxidants might improve the health status of TB patients and augment antibacterial TB chemotherapy.

Keywords

TNT; nicotinamide adenine dinucleotide; reactive oxygen species; necroptosis; macrophages

INTRODUCTION

Mycobacterium tuberculosis (Mtb), the etiological agent of Tuberculosis (TB), is the leading cause of death from a single infection agent worldwide. In 2017, Mtb infected more than 10 million people, resulting in over 1.3 million reported deaths in HIV-negative individuals and 300,000 additional deaths in HIV-positive individuals (WHO, 2018). The success of Mtb as a pathogen relies on its ability to avoid and manipulate the host immune response and to

persist in healthy individuals (Russell, Barry, & Flynn, 2010). A key mechanism used by Mtb to evade host defenses is its ability to trigger a necrotic cell death in infected host cells enabling rapid replication and dissemination (Behar, Divangahi, & Remold, 2010; Behar et al., 2011; Liu, Li, Xiang, & Xie, 2015). Recently, we showed that the outer membrane channel protein with necrosis-inducing Toxin (CpnT) is not only the main cytotoxicity factor of Mtb in macrophages, but also induces necrotic cell death (Danilchanka et al., 2014). CpnT contains two functional domains with different roles in Mtb pathogenesis. While the N-terminal domain is involved in nutrient acquisition across the outer membrane, the C-terminal domain, dubbed as the tuberculosis necrotizing toxin (TNT), is a NAD^+ glycohydrolase that depletes the cellular NAD^+ (Sun et al., 2015). Recently, we showed that TNT is the main molecular trigger of Mtb-induced macrophage necroptosis (Pajuelo et al., 2018). Necroptosis is a form of programmed necrosis canonically initiated by death receptor signaling-mediated activation of receptor-interacting serine-threonine kinase (RIPK) 1, RIPK3 and the effector molecule MLKL. Upon death receptor ligation, RIPK1 binds to RIPK3 through their homotypic interaction motif domains forming the necroptosome. The necroptosome then phosphorylates MLKL which inserts into the mitochondrial and cytoplasmic membranes leading to their lysis and the release of cellular contents (Newton & Manning, 2016; Vanden Berghe, Linkermann, Jouan-Lanhouet, Walczak, & Vandenabeele, 2014; Wang et al., 2014). Mtb shortcuts the activation of necroptosis by activating RIPK3 through TNT-dependent NAD^+ depletion bypassing death receptor and RIPK1 signaling (Pajuelo et al., 2018).

A hallmark of macrophage cell death induced by Mtb is the mitochondrial damage and extensive production of reactive oxygen species (ROS) (Amaral et al., 2016; Duan, Gan, Golan, & Remold, 2002; Zhao et al., 2017). Normally, low amounts of ROS are produced in mammalian cells as a byproduct of the electron transport chain (Murphy, 2009). However, excess ROS production in mitochondria at later stages of mycobacteria-induced necroptosis is a consequence of mitochondrial damage and dysfunction (Roca & Ramakrishnan, 2013; Zhao et al., 2017), causing oxidative damage to host cell proteins and membranes (Nunnari & Suomalainen, 2012; Orrenius, Gogvadze, & Zhivotovsky, 2007). While ROS production is a known consequence of necroptosis and is triggered by bacterial effectors such as pore forming toxins (Gonzalez-Juarbe et al., 2015), the contribution of TNT to ROS production in macrophages infected with Mtb is unknown. Furthermore, the finding that excess ROS can trigger necroptosis raised the possibility that ROS could accelerate and/or exacerbate necroptotic cell death in Mtb-infected macrophages (Zhang et al., 2017).

In this study, we examined the role of TNT in generation of oxidative stress in cells infected with Mtb. We show that the NAD^+ glycohydrolase activity of TNT is an important contributor to ROS production not only during Mtb infection of macrophages, but also when expressed in Jurkat-T cells, demonstrating that TNT is sufficient to induce lethal oxidative stress. In addition, Mtb induces ROS production through pathways other than TNT and in a necroptosis-independent manner. Importantly, NAD^+ replenishment and/or ROS scavenging reduce oxidative stress and efficiently protect macrophages from Mtb-induced cell death, revealing new avenues for host-directed TB chemotherapies.

RESULTS

TNT-induced ROS production promotes cell death and intracellular replication in macrophages infected with Mtb

In order to examine whether the TNT activity during infection of macrophages with Mtb leads to ROS production, we used a human monocyte cell line (THP-1) differentiated into macrophages as a model (Mendoza-Coronel & Castanon-Arreola, 2016; Riendeau & Kornfeld, 2003). THP-1 macrophages were infected with wild-type (wt) Mtb H37Rv, the *cpnT* deletion mutant and with the strains complemented with the wt *cpnT* gene (Mtb *cpnT*+*cpnT*) or with *cpnT* encoding a mutated, non-catalytic TNT$_{H790N/Q822K}$ domain (Mtb *cpnT*+*cpnT**) (Table 1). Mtb strains encoding wt *cpnT* increased ROS production in infected macrophages 24 h after infection, while strains lacking functional CpnT only started to accumulate ROS 48 h after infection (Fig. 1A), indicating that CpnT is an important factor inducing oxidative stress in macrophages. Strains producing wt CpnT increased ROS levels by two-fold compared with ROS generated by the non-catalytic TNT mutant 48 h after infection (p-value <0.01) (Fig. 1A), underlining the important role of NAD$^+$ hydrolysis by TNT for the increase in ROS production in Mtb-infected macrophages. Interestingly, the non-catalytic TNT mutant increased ROS production 48 h after infection compared with the uninfected macrophages (p-value <0.01), indicating the existence of ROS-generating pathways independent of the enzymatic activity of TNT (Fig. 1A).

To examine whether the TNT-induced ROS are indeed involved in cell death, we aimed to decrease ROS accumulation in Mtb-infected macrophages by treatment with the ROS scavenger N-acetyl-cysteine (NAC) (Amaral et al., 2016). As shown in Figure 1B, NAC reduced ROS accumulation in macrophages infected with Mtb for all strains. Importantly, decreasing ROS levels by NAC partially restored macrophage viability (Fig. 1C), indicating that the produced ROS are directly involved in cell death. In addition, ROS scavenging by NAC restricted the intracellular replication of wt Mtb and the complemented Mtb strains in macrophages (Fig. 1D). This difference in intracellular replication was not due to different phagocytosis since the number of phagocytosed bacteria was similar for all strains 4 h after infection (Fig. 1D). Replication of the Mtb strains producing functional *cpnT* within the first 48 h after infection appeared to be slightly faster than expected compared to the generation time of Mtb of ~20 h (Fig. 1C). This might be explained by the fact that macrophages engulf clumps of bacteria (Mahamed et al., 2017) which may segregate later leading to an underestimation of the initial CFU detected at 4 h after infection. It is also noteworthy that the Mtb strain producing non-catalytic TNT doubled within the first 48 h but NAC treatment did not affect its intracellular replication (Fig. 1D). The interpretation of the data for the *cpnT* strain is difficult since this strain lacks the N-terminal domain of CpnT, whose nutrientuptake activity is required for replication within macrophages (Danilchanka et al., 2014; Pajuelo et al., 2018). Therefore, it is likely that ROS production by CpnT-independent mechanisms is reduced in the *cpnT* strain. For this reason, we do not interpret the results obtained with the Mtb *cpnT* strain in this and in the subsequent experiments. NAC was used at a concentration that was not toxic for Mtb demonstrating that the observed phenotype is not a consequence of a direct bactericidal effect of NAC (Fig. 1E). Collectively,

these results indicate that the catalytic activity of TNT increases ROS levels in macrophages infected with Mtb promoting bacterial replication and macrophage cell death.

ROS accumulate downstream of necroptosis activation and mitochondrial depolarization

We recently described that necroptosis triggered by TNT in Mtb-infected macrophages is composed of three sequential molecular events: (i) TNT depletes the cytosolic NAD$^+$ pool, (ii) the necroptosis effectors RIPK3 and MLKL are activated, and (iii) mitochondria are depolarized via the mitochondrial permeability transition (MPT) pore leading to cell death (Pajuelo et al., 2018). The molecular mechanisms triggering mitochondrial damage and ROS production after activation of necroptosis by mycobacteria have been described (Roca & Ramakrishnan, 2013; Zhao et al., 2017). Although we showed that TNT is a major contributor to oxidative stress in macrophages, it is unknown how ROS are produced during the TNT-induced necroptotic pathway. In order to determine the origin of the TNT-induced ROS detected in macrophages infected with Mtb, we aimed to reverse or block the main molecular events of TNT-dependent necroptosis, i.e., NAD$^+$ depletion, activation of the necroptosis effectors RIPK3/MLKL and mitochondrial depolarization.

NAD$^+$ replenishment in THP-1 macrophages by nicotinamide supplementation, increases cellular NAD$^+$ levels and counters the TNT enzymatic activity, thereby alleviating the TNT-induced cytotoxicity (Pajuelo et al., 2018; Sun et al., 2015). Interestingly, nicotinamide reduced ROS levels in macrophages infected with Mtb expressing wt *cpnT*, but not in macrophages infected with *cpnT* mutant or Mtb producing the non-catalytic TNT mutant, indicating that the ROS production by TNT relies entirely on its NAD$^+$ glycohydrolase activity (Fig. 2A).

To determine the amount of ROS originating from necroptosis, we used GSK'872 and necrosulfonamide to inhibit RIPK3 and MLKL, respectively (Degterev et al., 2005; Kaiser et al., 2013). These necroptosis inhibitors efficiently protected THP-1 macrophages from necroptotic cell death induced by treatment with a combination of TNF-α, cycloheximide and carbobenzoxyvalyl-alanyl-aspartyl-[O-methyl]-fluoromethylketone (zVAD-fmk) (T/C/Z) as previously described (Cho et al., 2009; Park et al., 2018) (Fig. 2B). As expected, blocking necroptosis by inhibiting either RIPK3 or MLKL decreased cellular ROS accumulation demonstrating that necroptosis generates a significant amount of ROS in macrophages infected with Mtb (Fig. 2C). RIPK3 and MLKL inhibition also decreased ROS accumulation in cells infected with Mtb producing the non-catalytic TNT mutant, indicating that part of the ROS production in Mtb-infected macrophages is mediated by necroptosis, but independent of the NAD$^+$ glycohydrolase activity of TNT (Fig. 2C). Interestingly, the necroptosis-dependent ROS production appears to rely entirely on CpnT, since necroptosis inhibition had no effect on the *cpnT* mutant (Fig. 2C). However, this might be explained by the growth defect of the *cpnT* strain described above, which might compromise the production of other Mtb factors inducing necroptosis-dependent ROS in the Mtb *cpnT* strain, therefore overestimating the involvement of CpnT in the necroptosis-dependent ROS production.

The depolarization of mitochondria during TNT-induced necroptosis is mediated by the MPT pore (Pajuelo et al., 2018). The formation of the MPT pore in Mtb-infected

macrophages has been associated with ROS production (Zhao et al., 2017). We observed that inhibition of MPT pore formation by cyclosporin A (CsA), a selective inhibitor of cyclophilin D activity (Broekemeier & Pfeiffer, 1995; Gan et al., 2005), reduced the ROS produced by strains encoding a functional TNT protein by app. 65% (Fig. 2A), demonstrating that most of the observed ROS originated as a consequence of mitochondrial depolarization by the MPT pore. CsA also reduced ROS levels in macrophages infected with the non-catalytic TNT mutant strain, showing that TNT-independent ROS production also relies in MPT pore formation (Fig. 2A). Surprisingly, ROS level in macrophages infected with the *cpnT* mutant were not decreased by CsA (Fig. 2A), suggesting that the growth defect of the deletion mutant affect other Mtb ROS-inducing factors, as previously discussed (Pajuelo et al., 2018). Altogether, our results demonstrate that the TNT-dependent ROS are produced in mitochondria of macrophages infected with Mtb as a consequence of the formation of the MPT pore after NAD^+ depletion and activation of necroptosis.

The TNT protein is sufficient to induce lethal oxidative stress

In a recent report, we showed that TNT is sufficient to induce necroptosis in Jurkat-T cells (Pajuelo et al., 2018). This experimental model consists of a Jurkat-T cell line containing an integrated TetR-regulated *tnt* expression cassette (Jurkat 655-TNT) that is induced by doxycycline and enables a tight control of *tnt* expression (Danilchanka et al., 2014; Pajuelo et al., 2018; Sun et al., 2015). Here, we used the Jurkat 655-TNT cell line to examine the contribution of TNT to oxidative stress without the interference of confounding bacterial factors during an infection experiment. As expected, doxycycline treatment induced cell death in a time- and dose-dependent manner (Fig. 3A). In order to study the ROS-induced cell death in this model, we selected a doxycycline dose of 5 ng/ml that induces a 30–40% of cytotoxicity within 48–72 h (Fig. 3A). Induction of TNT production with 5 ng/ml of doxycycline increased ROS accumulation compared with non-treated cells (Fig. 3B), demonstrating that TNT induces oxidative stress without the aid of other mycobacterial factors. As expected, ROS levels were reduced when the cells were treated with the ROS scavenger NAC (Fig. 3B). ROS levels were also reduced by NAD^+ replenishment by nicotinamide and by preventing mitochondrial depolarization with CsA (Fig. 3B), confirming our previous conclusion derived from Mtb-infected macrophages that NAD^+ depletion by TNT is a major mechanism triggering ROS formation and that part of the produced ROS originates from mitochondrial depolarization by the MPT pore.

In order to study the role of ROS in the TNT-induced cell death in the Jurkat-T cell model, we analyzed the cell viability under a variety of conditions. Most importantly, ROS scavenging with NAC improved cell viability (Fig. 3C), indicating a direct role of ROS in TNT-induced cell death in Jurkat-T cells. NAD^+ replenishment by nicotinamide and protection of mitochondrial depolarization by CsA also protected from cell death (Fig. 3C). Altogether, these results demonstrate that TNT is sufficient to generate lethal oxidative stress. It is important to note these lethal effects of TNT are triggered by very low protein quantities (<10 ng) which are not detectable in a western blot (Fig. 3D).

NAD⁺ depletion is sufficient to induce ROS accumulation in macrophages

We recently showed that depletion of NAD^+ triggers necroptosis in macrophages when NAD^+ levels drop below a critical threshold (Pajuelo et al., 2018). In order to examine whether necroptosis triggered by the NAD^+ depletion independent of TNT involves the same molecular events than those induced by TNT, i.e. mitochondrial damage and ROS accumulation, we treated the THP-1 macrophages with FK866, an inhibitor of nicotinamide phosphoribosyl-transferase (NAMPT), a key enzyme in the NAD^+ salvage pathway (Hasmann & Schemainda, 2003). The mitochondrial membrane potential decreased in macrophages treated with 10 μM FK866 for 6 h, while lower concentrations had no effect (Fig. 4A). An increase in the ROS production was only observed when macrophages were treated with 10 μM FK866 (Fig. 4B), although we previously observed that 100 nM FK866 are sufficient to strongly reduce NAD^+ levels and induce necroptosis (Pajuelo et al., 2018). Furthermore, the cell death induced by FK866 was not restored with the ROS scavenger NAC (Fig. 4C), indicating that the ROS produced by FK866-induced NAD^+ depletion do not contribute in cell death.

Menadione-induced ROS do not enhance necroptosis by a positive feedback loop in macrophages

ROS have been shown to not only damage cell components, but also to promote RIPK1 autophosphorylation and initiate necroptosis (Zhang et al., 2017). Hence, we hypothesized that the ROS produced by TNT in macrophages might contribute to activate necroptosis in addition to NAD^+ depletion, thereby establishing a positive feedback loop. To examine whether ROS by themselves trigger necroptosis, we utilized menadione as a different ROS-inducing mechanism. Menadione is a quinone that is metabolized by reductive enzymes to an unstable semiquinone, which is oxidized again to quinone in the presence of molecular oxygen. During this redox cycle, reactive oxygen species such as superoxide and hydrogen peroxide are generated (Gerasimenko et al., 2002; Okada et al., 2005). We showed that menadione killed THP-1 cells in a dose- and time-dependent manner (Fig. 5A). For further experiments, we chose a concentration of 160 μM menadione since approximately half of the cells were dead after 8–10 h (Fig. 5A). Consistent with previous reports (Gerasimenko et al., 2002; Okada et al., 2005), 160 μM menadione strongly increased ROS levels (Fig. 5B). Treatment with the ROS scavenger NAC almost completely restored cell viability (Fig. 5C), indicating that ROS production is the lethal mechanism induced by menadione in these experiments and not induction of apoptosis (Bozic, Bidovec, Vizovisek, Dolenc, & Stoka, 2019) or other mechanism. In contrast, inhibition of necroptosis by necrostatin-1s (RIPK1), GSK'872 (RIPK3) and necrosulfonamide (MLKL) did not prevent the cell death induced by menadione (Fig. 5C), indicating that menadione induces macrophage cell death through ROS production in a necroptosis-independent manner. We also ruled out the involvement of mitochondrial depolarization in menadione-induced cell death, since blocking the formation of the MPT pore by CsA did not protect THP-1 cells (Fig. 5C). These results are in accordance with the observation that menadione-induced ROS formation does not depend on the necroptosis effectors or mitochondrial depolarization, since necroptosis inhibitors and CsA did not decrease ROS production, while supplementation with NAC efficiently reduced ROS accumulation (Fig. 5B). Taken together, these results indicate that ROS do not activate

necroptosis in THP-1 cells and do not establish a positive feedback loop for necroptosis activation in macrophages infected with Mtb.

DISCUSSION

Mitochondrial damage and increased ROS production are hallmarks of cells infected with mycobacteria (Amaral et al., 2016; Duan et al., 2002; Roca & Ramakrishnan, 2013; Zhao et al., 2017). In this study, we determined that Mtb increased ROS levels in infected THP-1 macrophages by three-fold and that the increased ROS production contributes to killing of the macrophages. Our analysis revealed four distinguishable molecular mechanisms of ROS production. Pathway 1 depends on the enzymatic activity of TNT, while pathway 2 is independent of TNT. Both of these pathways can be either dependent on necroptosis or not (Figure 6).

TNT-dependent pathways of ROS production

The enzymatic activity of TNT is a major contributor to ROS accumulation in macrophages infected by Mtb, accounting for approximately 50% of the ROS induced by Mtb in the macrophage (Fig. 1A, 1B). Our experiments showed that TNT-induced ROS are not dependent on necroptosis because the reduction of ROS levels by necroptosis inhibitors is similar in THP-1 macrophages infected with Mtb strains expressing wt TNT and the non-catalytic TNT mutant (Fig. 2C). However, TNT is an important molecular trigger of necroptosis mediated by RIPK3 and MLKL (Pajuelo et al., 2018), and these necroptosis effectors induce ROS production (Roca & Ramakrishnan, 2013; Xu et al., 2017; Zhao et al., 2017) (Fig. 6, **pathway 1a**). A possible explanation for these apparently contradictory findings might be that other TNT-independent mechanisms might be upregulated and compensate for the lack TNT, therefore masking the contribution of the TNT-induced necroptosis in ROS accumulation. We also observed that TNT triggers other mechanisms of ROS production when necroptosis is inhibited (Figs. 2c, 6, **pathway 1b**). Such a mechanism could be mediated by sirtuins, NAD^+-consuming enzymes involved in different homeostasis processes (Chang & Guarente, 2014). Two proteins of this family, SIRT1 and SIRT3, have been shown to promote the expression of genes with antioxidant activity, such as manganese superoxide dismutase, glutathione peroxidase and catalase (Merksamer et al., 2013; Salminen, Kaarniranta, & Kauppinen, 2013). It is conceivable that NAD^+ depletion by TNT may impair the antioxidant cellular response to ROS thereby increasing ROS levels. In addition, depletion of cytosolic NAD^+ quickly decreases the mitochondrial NAD^+ pool (Cambronne et al., 2016), probably affecting the activity of SIRT3 in mitochondria which is required for mitochondrial function (Chang & Guarente, 2014). Obviously, more work is needed to examine these hypotheses. The importance of NAD^+ hydrolysis by TNT in ROS production is supported by experiments using the Jurkat-T cell line expressing *tnt* (Danilchanka et al., 2014; Pajuelo et al., 2018). We found that TNT alone induces lethal quantities of ROS, demonstrating that NAD^+ hydrolysis by TNT alone is sufficient to induce the major molecular events in macrophages infected with Mtb including triggering necroptotic cell death, mitochondrial damage (Pajuelo et al., 2018) and oxidative stress.

TNT-independent pathways of ROS production

Approximately half of the ROS produced in THP-1 macrophages infected with Mtb in our study was independent of the activity of TNT. One of these mechanisms relies on activation of necroptosis in a TNT-independent manner (Fig. 6, **pathway 2a**), as indicated by reduced ROS levels in the presence of GSK'872 and necrosulfonamide in macrophages infected with the non-catalytic mutant of TNT (Fig. 2C). A fourth mechanism of ROS production in macrophages infected with Mtb is independent of both TNT and necroptosis, as evidenced by the fact that some ROS accumulate in the absence of necroptosis and the enzymatic activity of TNT (Figs. 2C, 6, **pathway 2b**). Examples of Mtb factors that might increase ROS production are those known to target mitochondria and induce mitochondria depolarization are the PE_PGRS33 protein, that colocalizes to the mitochondria to induce cell death by apoptosis and necrosis (Cadieux et al., 2011), and the Mtb heparin-binding hemagglutinin (HBHA), that is targeted to mitochondria, where it dissipates the membrane potential and releases cytochrome c (Sohn et al., 2011). Moreover, an *in silico* approach identified 19 Mtb proteins that could target host cell mitochondria, some of whom are well known virulence factors such as the p27 protein (Moreno-Altamirano et al., 2012). Additionally, Mtb may generate ROS by other pathways such as ferroptosis, a necrotic-like cell death that is associated with increased free iron, which generates ROS by the Fenton reaction (Amaral et al., 2019). It is likely that some ROS are produced by NAD^+ depletion independent of TNT. This conclusion is supported by the finding that Mtb infection causes a significant drop in NAD^+ levels even in the absence of TNT (Pajuelo et al., 2018). Indeed, NAD^+ depletion itself, induced by the NAMPT inhibitor FK866, was shown to trigger necroptosis (Pajuelo et al., 2018) and was found to increase ROS production (Fig. 4B). However, even high FK866 concentrations produced only modest amounts of ROS. This is in contrast to the very low TNT concentrations needed to trigger ROS production in Jurkat T cells (Fig. 4). This could be due to the fact one TNT molecule can hydrolyse 16 NAD^+ molecules per second (Tak et al., 2019) and/or might reflect the different mechanisms of NAD^+ depletion. While NAD^+ hydrolysis by TNT produces nicotinamide and ADP-ribose (Sun et al., 2015), inhibition of NAMPT by FK866 prevents the synthesis of NAD^+ and NAD^+ hydrolysis products such as ADP ribose are not accumulated. ADP-ribose is a signaling molecule involved in important cellular processes such as regulation of calcium levels (Perraud et al., 2001; Wei, Graeff, & Yue, 2014). Increased calcium levels have been related with the generation of ROS (Adam-Vizi & Starkov, 2010), indicating why ROS production by TNT is higher than that by NAMPT inhibition using FK866.

Does ROS production by TNT trigger necroptosis in a positive feedback loop?

Given the high amount of ROS produced by the enzymatic activity of TNT, and the fact that ROS induce necroptosis in other cell types (Zhang et al., 2017), we hypothesized that the TNT-induced ROS enhance necroptosis activation in Mtb-infected macrophages, establishing a positive feedback loop for necroptosis induction. For this purpose, we induced ROS formation with menadione to study their role in macrophage necroptosis. Although apoptotic and necrotic features have been related with menadione-induced cell death, the MPT pore and apoptosis mediators have been ruled out by studies using genetic tools (Criddle et al., 2006; Gerasimenko et al., 2002; Loor et al., 2010). Instead, PARP activation

is a major mediator in the cell death triggered by menadione-induced oxidative stress (Loor et al., 2010). In this work, we found that the macrophage cell death induced by menadione was mediated by its ROS production but was independent of necroptosis and mitochondrial depolarization, in accordance with previous studies showing that blocking MPT pore formation or inhibition of RIPK1 by necrostatin-1s did not reduce cell death elicited by menadione (Degterev et al., 2005; Loor et al., 2010; Xu et al., 2007). These results indicate that ROS by themselves do not trigger necroptosis in macrophages and that the TNT-induced ROS do not establish a positive feedback loop for necroptosis activation in infected macrophages.

Origin of ROS produced in Mtb-infected macrophages.

Most ROS generated by Mtb originate from mitochondria, as shown by the large impact of the inhibition of the MPT pore by CsA. The protection conferred by CsA had less effect in macrophages infected with the non-catalytic mutant compared with those infected with the wt Mtb strain (Fig. 2A), indicating that much of the mitochondrial ROS is dependent on the catalytic activity of TNT. This finding is consistent with our previous work describing the severe mitochondrial damage induced by TNT during macrophage necroptosis (Pajuelo et al., 2018) and recent work describing the RIPK3-dependent formation of the MPT pore in mitochondria as a major source of ROS in Mtb-infected macrophages (Zhao et al., 2017). The MPT pore enables ROS to leave the mitochondria and cause oxidative damage to host cell proteins and membranes (Nunnari & Suomalainen, 2012; Orrenius et al., 2007). A similar mechanism was also observed in macrophages infected with *Mycobacterium marinum* (Roca & Ramakrishnan, 2013). It is important to note that the contribution of non-mitochondrial ROS to Mtb-induced cell death in infected macrophages is unclear and, hence, is not represented in Figure 6.

Conclusions

We observed that N-acetyl-cysteine, one of the most widely studied antioxidants (Ezerina, Takano, Hanaoka, Urano, & Dick, 2018), not only decreased ROS accumulation but also protected Mtb-infected macrophages from cell death and restricted intracellular replication. On a systemic level, the overproduction of ROS in TB patients induces oxidative stress in the lungs and promotes tissue injury and inflammation in TB patients (Awodele, Olayemi, Nwite, & Adeyemo, 2012; Mittal, Siddiqui, Tran, Reddy, & Malik, 2014; Rajopadhye, Mukherjee, Chowdhary, & Dandekar, 2017; Shastri et al., 2018). Treatment with antioxidants to counteract tissue damage indeed decreased pathology and mycobacterial load in lungs of mice infected with Mtb underlining the key role of excess ROS production in TB pathogenesis (Amaral et al., 2016; Palanisamy et al., 2011). In this regard, the strong contribution of TNT to ROS production in Mtb-infected macrophages, as shown in this study, reveals NAD^+ replenishment as an alternative strategy to decrease oxidative stress in TB patients. In conclusion, our study suggests that combining anti-oxidant therapies with NAD^+ replenishment could improve the health status of TB patients.

MATERIAL AND METHODS

Bacterial strains and culture conditions

Mtb H37Rv and its derivative strains were grown in Middlebrook 7H9 medium (Difco) supplemented with 0.5% glycerol, 0.02% Tyloxapol and 10% OADC (Remel) or in Middlebrook 7H10 plates supplemented with 0.5% glycerol and 10% OADC (Remel). All bacterial strains used are shown in the Table 1.

Infection of macrophages

Mtb strains were harvested in mid-log phase (OD_{600} of 0.6). Macrophages were infected with the Mtb strains at a multiplicity of infection (MOI) of 10:1 for 4 h. Macrophage monolayers were incubated with media containing 20 μg/ml gentamycin for 1 h to kill extracellular bacteria and then kept in media without antibiotics. When macrophages were treated with a compound, the chemicals were added to the media 1 h before the infection and were kept in media for the rest of the experiment. In all the experiments involving macrophages, both floating and attached macrophages were collected and analyzed.

Cell culture

Human THP-1 monocytes (ATCC TIB-202) were propagated in RPMI-1640 (HyClone) supplemented with 10% FBS (Gibco), 10 mM HEPES (HyClone), 2 mM L-glutamine (HyClone), 1x non-essential aminoacids (HyClone), 100 U/ml penicillin (Gibco), 100 μg/ml streptomycin (Gibco) and 250 ng/ml amphotericin B (Gibco). The day prior to infection, THP-1 monocytes were seeded on cell culture-treated plates and differentiated for 24 h into macrophage-like cells with 20 ng/mL 12-phorbol 13-myristate acetate (PMA) (Sigma). The Jurkat 655-TNT cell line stably expressing a doxycycline-controlled combined repressor/ activator switch featuring the second generation Tet-transregulators rtTA2[S]-M2 and tTS[D]-PP encoding TNT (Danilchanka et al., 2014) was maintained in RPMI-1640 medium supplemented with the same reagents than THP-1 cells. All cells were grown in a 37°C humidified incubator at 5% CO_2. Cell lines were routinely tested for mycoplasma contamination as described elsewhere (Young, Sung, Stacey, & Masters, 2010).

Mitochondrial membrane potential

The status of the mitochondrial membrane potential in macrophages was determined with the MITO-ID Membrane potential cytotoxicity kit (Enzo) as described by the manufacturer. The MITO-ID reagent uses a lipophilic cationic dye based on JC-1 (Smiley et al., 1991) that accumulates as orange-red fluorescent J-aggregates in mitochondria. The fluorescence was recorded with a BioTek Synergy HT plate reader (BioTek).

ROS measurement

ROS accumulation in cells was assessed with 2',7'-dichlorodihydrofluorescein diacetate (H_2DCFDA) (ThermoFisher), a cell-permeant ROS indicator that upon cleavage of the acetate group by intracellular esterases and oxidation is converted to the highly fluorescent 2',7'-dichlorofluorescein (DCF), as previously described (Gonzalez-Juarbe et al., 2015). The fluorescence was recorded with a BioTek Synergy HT plate reader (BioTek).

Cell viability

The cell viability of macrophages was assessed with the Cell Titter-Glo Luminescent Viability Assay (Promega), a luciferase-based that determines the number of viable cells in culture by quantifying ATP. The luminescence was recorded with a BioTek Synergy HT plate reader (BioTek). For some experiments, macrophage viability was measured by trypan blue staining (Strober, 2015).

Purification of TNT protein

Wild-type TNT protein was purified from E. coli BL21 (DE3) cells containing the plasmids pML1995 (Table S1) as previously described (Sun et al., 2015).

Chemicals

When required, the following chemicals were added to the cells 1 h prior and kept for the rest of the experiment at the stated concentration in the figure legends; nicotinamide (Sigma), cyclosporin A (CsA) (Sigma), necrostatin-1s (Nec-1s) (Millipore), GSK'872 (Milipore), necrosulfonamide (NSA) (Tocris Bioscience), FK866 (Selleckchem, Sigma), menadione (MP Biomedicals) and N-acetyl-cysteine (NAC) (Sigma). All compounds were dissolved in DMSO except for nicotinamide. Macrophages were treated with an equivalent DMSO concentration as a negative control and showed no differences in mitochondrial membrane potential, cell viability, and ROS production compared to non-treated macrophages (data not shown).

Intracellular survival in macrophages

Survival of Mtb in THP-1 macrophages was performed as previously described (Danilchanka et al., 2014). Briefly, THP-1 macrophages were seeded in 24-well plates (5×10^5 cells/well) and infected as described above. Since it has been shown that Mtb replicates in dead, necrotic macrophages (Lerner et al., 2017), and that macrophages undergoing cell death detach from the well surface, we analyzed both attached and floating macrophages in these experiments. At 4 h and 48 h time points, attached and floating macrophages (collected by centrifugation, 800 rpm, 5 min) were lysed in 0.025% SDS for 5 minutes at room temperature and serial dilutions were plated on 7H10 agar plates supplemented with 0.5% glycerol, 10% OADC and kanamycin (for complemented strains). CFU counts were performed after 3 weeks of incubation at 37°C. The intracellular survival is presented as the CFU per ml.

Statistical analysis

The experiments were performed three times independently (three independent biological replicates). Within each biological replicate, at least three technical replicates were performed. The data are presented as the mean ± standard error of the mean of the biological replicates; p-values were calculated using the One-way or Two-way ANOVA with Bonferroni's correction and a p-value of <0.01 was considered to be significant.

ACKNOWLEDGMENTS

REFERENCES

Adam-Vizi V, & Starkov AA (2010). Calcium and mitochondrial reactive oxygen species generation: how to read the facts. J Alzheimers Dis, 20 Suppl 2, S413–426. doi:10.3233/JAD-2010-100465 [PubMed: 20421693]

Amaral EP, Conceicao EL, Costa DL, Rocha MS, Marinho JM, Cordeiro-Santos M, . . . Andrade BB (2016). N-acetyl-cysteine exhibits potent anti-mycobacterial activity in addition to its known anti-oxidative functions. BMC Microbiol, 16(1), 251. doi:10.1186/s12866-016-0872-7 [PubMed: 27793104]

Amaral EP, Costa DL, Namasivayam S, Riteau N, Kamenyeva O, Mittereder L, . . . Sher A (2019). A major role for ferroptosis in *Mycobacterium tuberculosis*-induced cell death and tissue necrosis. J Exp Med, 216(3), 556–570. doi:10.1084/jem.20181776 [PubMed: 30787033]

Awodele O, Olayemi SO, Nwite JA, & Adeyemo TA (2012). Investigation of the levels of oxidative stress parameters in HIV and HIV-TB co-infected patients. J Infect Dev Ctries, 6(1), 79–85. [PubMed: 22240433]

Behar SM, Divangahi M, & Remold HG (2010). Evasion of innate immunity by *Mycobacterium tuberculosis*: is death an exit strategy? Nat Rev Microbiol, 8(9), 668–674. doi:10.1038/nrmicro2387 [PubMed: 20676146]

Behar SM, Martin CJ, Booty MG, Nishimura T, Zhao X, Gan HX, . . . Remold HG (2011). Apoptosis is an innate defense function of macrophages against *Mycobacterium tuberculosis*. Mucosal Immunol, 4(3), 279–287. doi:10.1038/mi.2011.3 [PubMed: 21307848]

Bozic J, Bidovec K, Vizovisek M, Dolenc I, & Stoka V (2019). Menadione-induced apoptosis in U937 cells involves Bid cleavage and stefin B degradation. J Cell Biochem, 120(6), 10662–10669. doi:10.1002/jcb.28356 [PubMed: 30652348]

Broekemeier KM, & Pfeiffer DR (1995). Inhibition of the mitochondrial permeability transition by cyclosporin A during long time frame experiments: relationship between pore opening and the activity of mitochondrial phospholipases. Biochemistry, 34(50), 16440–16449. [PubMed: 8845372]

Cadieux N, Parra M, Cohen H, Maric D, Morris SL, & Brennan MJ (2011). Induction of cell death after localization to the host cell mitochondria by the Mycobacterium tuberculosis PE_PGRS33 protein. Microbiology, 157(Pt 3), 793–804. doi:10.1099/mic.0.041996-0 [PubMed: 21081760]

Cambronne XA, Stewart ML, Kim D, Jones-Brunette AM, Morgan RK, Farrens DL, . . . Goodman RH (2016). Biosensor reveals multiple sources for mitochondrial NAD(+). Science, 352(6292), 1474–1477. doi:10.1126/science.aad5168 [PubMed: 27313049]

Chang HC, & Guarente L (2014). SIRT1 and other sirtuins in metabolism. Trends Endocrinol Metab, 25(3), 138–145. doi:10.1016/j.tem.2013.12.001 [PubMed: 24388149]

Cho YS, Challa S, Moquin D, Genga R, Ray TD, Guildford M, & Chan FK (2009). Phosphorylationdriven assembly of the RIP1-RIP3 complex regulates programmed necrosis and virus-induced inflammation. Cell, 137(6), 1112–1123. doi:10.1016/j.cell.2009.05.037 [PubMed: 19524513]

Criddle DN, Gillies S, Baumgartner-Wilson HK, Jaffar M, Chinje EC, Passmore S, . . . Petersen OH (2006). Menadione-induced reactive oxygen species generation via redox cycling promotes apoptosis of murine pancreatic acinar cells. J Biol Chem, 281(52), 40485–40492. doi:10.1074/jbc.M607704200 [PubMed: 17088248]

Danilchanka O, Sun J, Pavlenok M, Maueroder C, Speer A, Siroy A, . . . Niederweis M (2014). An outer membrane channel protein of *Mycobacterium tuberculosis* with exotoxin activity. Proc Natl Acad Sci U S A, 111(18), 6750–6755. doi:10.1073/pnas.1400136111 [PubMed: 24753609]

Degterev A, Huang Z, Boyce M, Li Y, Jagtap P, Mizushima N, . . . Yuan J (2005). Chemical inhibitor of nonapoptotic cell death with therapeutic potential for ischemic brain injury. Nat Chem Biol, 1(2), 112–119. doi:10.1038/nchembio711 [PubMed: 16408008]

Duan L, Gan H, Golan DE, & Remold HG (2002). Critical role of mitochondrial damage in determining outcome of macrophage infection with Mycobacterium tuberculosis. J Immunol, 169(9), 5181–5187. [PubMed: 12391235]

Ezerina D, Takano Y, Hanaoka K, Urano Y, & Dick TP (2018). N-Acetyl Cysteine Functions as a Fast-Acting Antioxidant by Triggering Intracellular H2S and Sulfane Sulfur Production. Cell Chem Biol, 25(4), 447–459 e444. doi:10.1016/j.chembiol.2018.01.011 [PubMed: 29429900]

Gan H, He X, Duan L, Mirabile-Levens E, Kornfeld H, & Remold HG (2005). Enhancement of antimycobacterial activity of macrophages by stabilization of inner mitochondrial membrane potential. J Infect Dis, 191(8), 1292–1300. doi:10.1086/428906 [PubMed: 15776376]

Gerasimenko JV, Gerasimenko OV, Palejwala A, Tepikin AV, Petersen OH, & Watson AJ (2002). Menadione-induced apoptosis: roles of cytosolic Ca(2+) elevations and the mitochondrial permeability transition pore. J Cell Sci, 115(Pt 3), 485–497. [PubMed: 11861756]

Gonzalez-Juarbe N, Gilley RP, Hinojosa CA, Bradley KM, Kamei A, Gao G, . . . Orihuela CJ (2015). Pore-Forming Toxins Induce Macrophage Necroptosis during Acute Bacterial Pneumonia. PLoS Pathog, 11(12), e1005337. doi:10.1371/journal.ppat.1005337 [PubMed: 26659062]

Hasmann M, & Schemainda I (2003). FK866, a highly specific noncompetitive inhibitor of nicotinamide phosphoribosyltransferase, represents a novel mechanism for induction of tumor cell apoptosis. Cancer Res, 63(21), 7436–7442. [PubMed: 14612543]

Kaiser WJ, Sridharan H, Huang C, Mandal P, Upton JW, Gough PJ, . . . Mocarski ES (2013). Toll-like receptor 3-mediated necrosis via TRIF, RIP3, and MLKL. J Biol Chem, 288(43), 31268–31279. doi:10.1074/jbc.M113.462341 [PubMed: 24019532]

Lerner TR, Borel S, Greenwood DJ, Repnik U, Russell MR, Herbst S, . . . Gutierrez MG (2017). *Mycobacterium tuberculosis* replicates within necrotic human macrophages. J Cell Biol, 216(3), 583–594. doi:10.1083/jcb.201603040 [PubMed: 28242744]

Liu M, Li W, Xiang X, & Xie J (2015). *Mycobacterium tuberculosis* effectors interfering host apoptosis signaling. Apoptosis, 20(7), 883–891. doi:10.1007/s10495-015-1115-3 [PubMed: 25840680]

Loor G,Kondapalli J, Schriewer JM, Chandel NS, Vanden Hoek TL, & Schumacker PT (2010). Menadione triggers cell death through ROS-dependent mechanisms involving PARP activation without requiring apoptosis. Free Radic Biol Med, 49(12), 1925–1936. doi:10.1016/j.freeradbiomed.2010.09.021 [PubMed: 20937380]

Mahamed D, Boulle M, Ganga Y, Mc Arthur C, Skroch S, Oom L, . . . Sigal A (2017). Intracellular growth of Mycobacterium tuberculosis after macrophage cell death leads to serial killing of host cells. Elife, 6. doi:10.7554/eLife.22028

Mendoza-Coronel E, & Castanon-Arreola M (2016). Comparative evaluation of in vitro human macrophage models for mycobacterial infection study. Pathog Dis, 74(6). doi:10.1093/femspd/ftw052

Merksamer PI, Liu Y, He W, Hirschey MD, Chen D, & Verdin E (2013). The sirtuins, oxidative stress and aging: an emerging link. Aging (Albany NY), 5(3), 144–150. doi:10.18632/aging.100544 [PubMed: 23474711]

Mittal M, Siddiqui MR, Tran K, Reddy SP, & Malik AB (2014). Reactive oxygen species in inflammation and tissue injury. Antioxid Redox Signal, 20(7), 1126–1167. doi:10.1089/ars.2012.5149 [PubMed: 23991888]

Moreno-Altamirano MM, Paredes-Gonzalez IS, Espitia C, Santiago-Maldonado M, Hernandez-Pando R, & Sanchez-Garcia FJ (2012). Bioinformatic identification of Mycobacterium tuberculosis proteins likely to target host cell mitochondria: virulence factors? Microb Inform Exp, 2(1), 9. doi:10.1186/2042-5783-2-9 [PubMed: 23259719]

Murphy MP (2009). How mitochondria produce reactive oxygen species. Biochem J, 417(1), 1–13. doi:10.1042/BJ20081386 [PubMed: 19061483]

Newton K, & Manning G (2016). Necroptosis and Inflammation. Annu Rev Biochem, 85, 743–763. doi:10.1146/annurev-biochem-060815-014830 [PubMed: 26865533]

Nunnari J, & Suomalainen A (2012). Mitochondria: in sickness and in health. Cell, 148(6), 1145–1159. doi:10.1016/j.cell.2012.02.035 [PubMed: 22424226]

Okada Y, Sakai H, Kohiki E, Suga E, Yanagisawa Y, Tanaka K, . . . Ikeda JE (2005). A dopamine D4 receptor antagonist attenuates ischemia-induced neuronal cell damage via upregulation of neuronal apoptosis inhibitory protein. J Cereb Blood Flow Metab, 25(7), 794–806. doi:10.1038/sj.jcbfm. 9600078 [PubMed: 15729293]

Orrenius S, Gogvadze V, & Zhivotovsky B (2007). Mitochondrial oxidative stress: implications for cell death. Annu Rev Pharmacol Toxicol, 47, 143–183. doi:10.1146/annurev.pharmtox. 47.120505.105122 [PubMed: 17029566]

Pajuelo D, Gonzalez-Juarbe N, Tak U, Sun J, Orihuela CJ, & Niederweis M (2018). NAD(+) Depletion Triggers Macrophage Necroptosis, a Cell Death Pathway Exploited by Mycobacterium tuberculosis. Cell Rep, 24(2), 429–440. doi:10.1016/j.celrep.2018.06.042 [PubMed: 29996103]

Palanisamy GS, Kirk NM, Ackart DF, Shanley CA, Orme IM, & Basaraba RJ (2011). Evidence for oxidative stress and defective antioxidant response in guinea pigs with tuberculosis. PLoS One, 6(10), e26254. doi:10.1371/journal.pone.0026254 [PubMed: 22028843]

Park HH, Park SY, Mah S, Park JH, Hong SS, Hong S, & Kim YS (2018). HS-1371, a novel kinase inhibitor of RIP3-mediated necroptosis. Exp Mol Med, 50(9), 125. doi:10.1038/s12276-018-01528 [PubMed: 30237400]

Perraud AL, Fleig A, Dunn CA, Bagley LA, Launay P, Schmitz C, . . . Scharenberg AM (2001). ADP-ribose gating of the calcium-permeable LTRPC2 channel revealed by Nudix motif homology. Nature, 411(6837), 595–599. doi:10.1038/35079100 [PubMed: 11385575]

Rajopadhye SH, Mukherjee SR, Chowdhary AS, & Dandekar SP (2017). Oxidative Stress Markers in Tuberculosis and HIV/TB Co-Infection. J Clin Diagn Res, 11(8), BC24–BC28. doi:10.7860/ JCDR/2017/28478.10473

Riendeau CJ, & Kornfeld H (2003). THP-1 cell apoptosis in response to Mycobacterial infection. Infect Immun, 71(1), 254–259. [PubMed: 12496173]

Roca FJ, & Ramakrishnan L (2013). TNF dually mediates resistance and susceptibility to mycobacteria via mitochondrial reactive oxygen species. Cell, 153(3), 521–534. doi:10.1016/j.cell. 2013.03.022 [PubMed: 23582643]

Russell DG, Barry CE 3rd, & Flynn JL (2010). Tuberculosis: what we don't know can, and does, hurt us. Science, 328(5980), 852–856. doi:10.1126/science.1184784 [PubMed: 20466922]

Salminen A, Kaarniranta K, & Kauppinen A (2013). Crosstalk between Oxidative Stress and SIRT1: Impact on the Aging Process. Int J Mol Sci, 14(2), 3834–3859. doi:10.3390/ijms14023834 [PubMed: 23434668]

Shastri MD, Shukla SD, Chong WC, Dua K, Peterson GM, Patel RP, . . . O'Toole RF (2018). Role of Oxidative Stress in the Pathology and Management of Human Tuberculosis. Oxid Med Cell Longev, 2018, 7695364. doi:10.1155/2018/7695364 [PubMed: 30405878]

Smiley ST, Reers M, Mottola-Hartshorn C, Lin M, Chen A, Smith TW, . . . Chen LB (1991). Intracellular heterogeneity in mitochondrial membrane potentials revealed by a J-aggregateforming lipophilic cation JC-1. Proc Natl Acad Sci U S A, 88(9), 3671–3675. [PubMed: 2023917]

Sohn H, Kim JS, Shin SJ, Kim K, Won CJ, Kim WS, . . . Kim HJ (2011). Targeting of Mycobacterium tuberculosis heparin-binding hemagglutinin to mitochondria in macrophages. PLoS Pathog, 7(12), e1002435. doi:10.1371/journal.ppat.1002435 [PubMed: 22174691]

Strober W (2015). Trypan Blue Exclusion Test of Cell Viability. Curr Protoc Immunol, 111, A3 B 1–3. doi:10.1002/0471142735.ima03bs111 [PubMed: 26529666]

Sun, Siroy A, Lokareddy RK, Speer A, Doornbos KS, Cingolani G, & Niederweis M (2015). The tuberculosis necrotizing toxin kills macrophages by hydrolyzing NAD. Nat Struct Mol Biol, 22(9), 672–678. doi:10.1038/nsmb.3064 [PubMed: 26237511]

Tak U, Vlach J, Garza-Garcia A, William D, Danilchanka O, de Carvalho LPS, . . . Niederweis M (2019). The tuberculosis necrotizing toxin is an NAD(+) and NADP(+) glycohydrolase with distinct enzymatic properties. J Biol Chem, 294(9), 3024–3036. doi:10.1074/jbc.RA118.005832 [PubMed: 30593509]

Vanden Berghe T, Linkermann A, Jouan-Lanhouet S, Walczak H, & Vandenabeele P (2014). Regulated necrosis: the expanding network of non-apoptotic cell death pathways. Nat Rev Mol Cell Biol, 15(2), 135–147. doi:10.1038/nrm3737 [PubMed: 24452471]

Wang H, Sun L, Su L, Rizo J, Liu L, Wang LF, . . . Wang X (2014). Mixed lineage kinase domain-like protein MLKL causes necrotic membrane disruption upon phosphorylation by RIP3. Mol Cell, 54(1), 133–146. doi:10.1016/j.molcel.2014.03.003 [PubMed: 24703947]

Wei W, Graeff R, & Yue J (2014). Roles and mechanisms of the CD38/cyclic adenosine diphosphate ribose/Ca(2+) signaling pathway. World J Biol Chem, 5(1), 58–67. doi:10.4331/wjbc.v5.i1.58 [PubMed: 24600514]

WHO. (2018). Global Tuberculosis Report.

Xu, Chua CC, Kong J, Kostrzewa RM, Kumaraguru U, Hamdy RC, & Chua BH (2007). Necrostatin1 protects against glutamate-induced glutathione depletion and caspase-independent cell death in HT-22 cells. J Neurochem, 103(5), 2004–2014. doi:10.1111/j.1471-4159.2007.04884.x [PubMed: 17760869]

Xu, Xu M, Tian Y, Yu Q, Zhao Y, Chen X, . . . Hu T (2017). Matrine induces RIP3-dependent necroptosis in cholangiocarcinoma cells. Cell Death Discov, 3, 16096. doi:10.1038/cddiscovery. 2016.96 [PubMed: 28179994]

Young L, Sung J, Stacey G, & Masters JR (2010). Detection of Mycoplasma in cell cultures. Nat Protoc, 5(5), 929–934. doi:10.1038/nprot.2010.43 [PubMed: 20431538]

Zhang Y, Su SS, Zhao S, Yang Z, Zhong CQ, Chen X, . . . Han J (2017). RIP1 autophosphorylation is promoted by mitochondrial ROS and is essential for RIP3 recruitment into necrosome. Nat Commun, 8, 14329. doi:10.1038/ncomms14329 [PubMed: 28176780]

Zhao, Khan N, Gan H, Tzelepis F, Nishimura T, Park SY, . . . Remold HG (2017). Bcl-xL mediates RIPK3-dependent necrosis in *M. tuberculosis*-infected macrophages. Mucosal Immunol, 10(6), 1553–1568. doi:10.1038/mi.2017.12 [PubMed: 28401933]
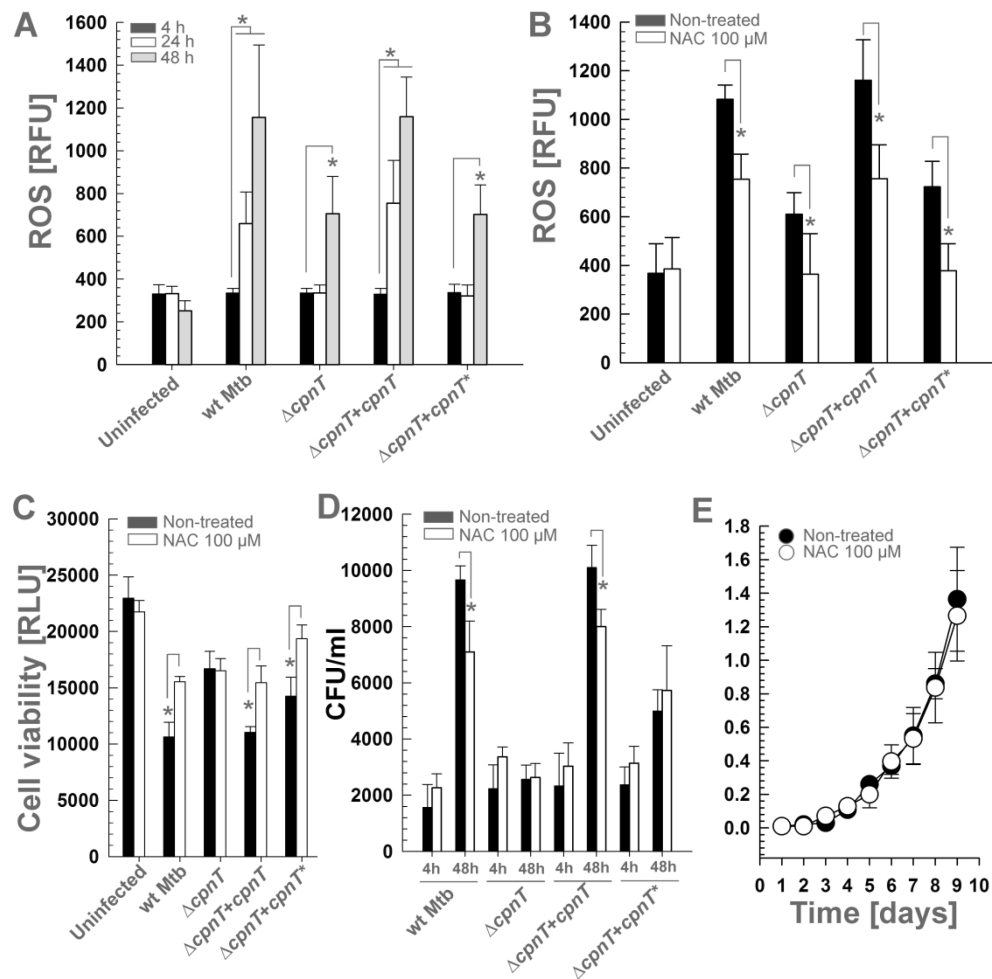
TNT-induced reactive oxygen species mediate macrophage cell death

Figure 1. TNT-induced reactive oxygen species mediate macrophage cell death.
THP-1 macrophages were infected with Mtb strains at an MOI of 10:1 and treated with N-acetylcysteine (NAC, 100 μM) when indicated. ROS levels were measured with the fluorescent probe H_2DCFDA at **(A)** 4, 24 and 48 h or **(B)** 48 h post-infection. **(C)** Cell viability of infected macrophages was measured 48 h after infection as the total ATP content with a luminescent ATP detection assay kit. **(D)** The Mtb intracellular growth in infected macrophages was measured at 4 h and 48 h post-infection and expressed as CFU per ml. **(E)** Wt Mtb H37Rv was grown in Middlebrook 7H9 medium with 0.5% glycerol, 0.02% Tyloxapol and 10% OADC and supplemented with N-acetyl-cysteine (NAC, 100 μM). The OD_{600} was measured at the indicated time points. Asterisks indicate significant differences (p-value<0.01, calculated using the Two-way ANOVA with Bonferroni's correction) compared with the indicated conditions. Data are represented as mean ± SEM.
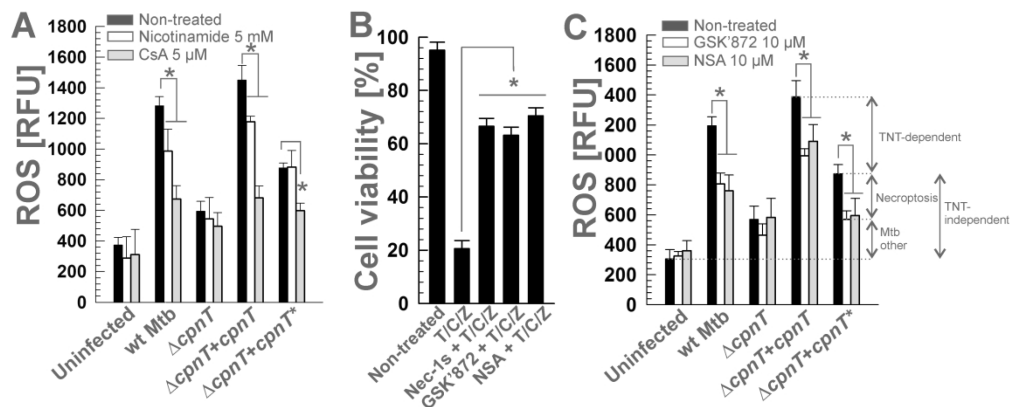
TNT-induced ROS accumulation occurs downstream NAD+ depletion, necroptosis activation and mitochondrial damage

Figure 2. TNT-induced ROS accumulation occurs downstream NAD$^+$ depletion, necroptosis activation and mitochondrial damage.

THP-1 macrophages were treated with **(A)** nicotinamide (5 mM) or cyclosporin A (CsA, 5 μM) and **(C)** the RIPK3 inhibitor GSK´872 (10 μM) or the MLKL inhibitor necrosulfonamide (NSA, 10 μM), and infected with Mtb strains at an MOI of 10:1 for 48 h. ROS levels (measured with the fluorescent probe H$_2$DCFDA) were analyzed. **(B)** THP-1 macrophages were treated with necrostatin-1s (Nec-1s, 10 μM), GSK'872 (10 μM), necrosulfonamide (NSA, 10 μM) and/or TNF-a, cycloheximide, and zVAD-fmk (T/C/Z) (Cho et al., 2009), and cell viability was measured by trypan blue. Asterisks indicate significant differences (p-value<0.01, calculated using the One-way [B] or Two-way [A, C] ANOVA with Bonferroni's correction) compared with the indicated conditions. Data are represented as mean ± SEM.
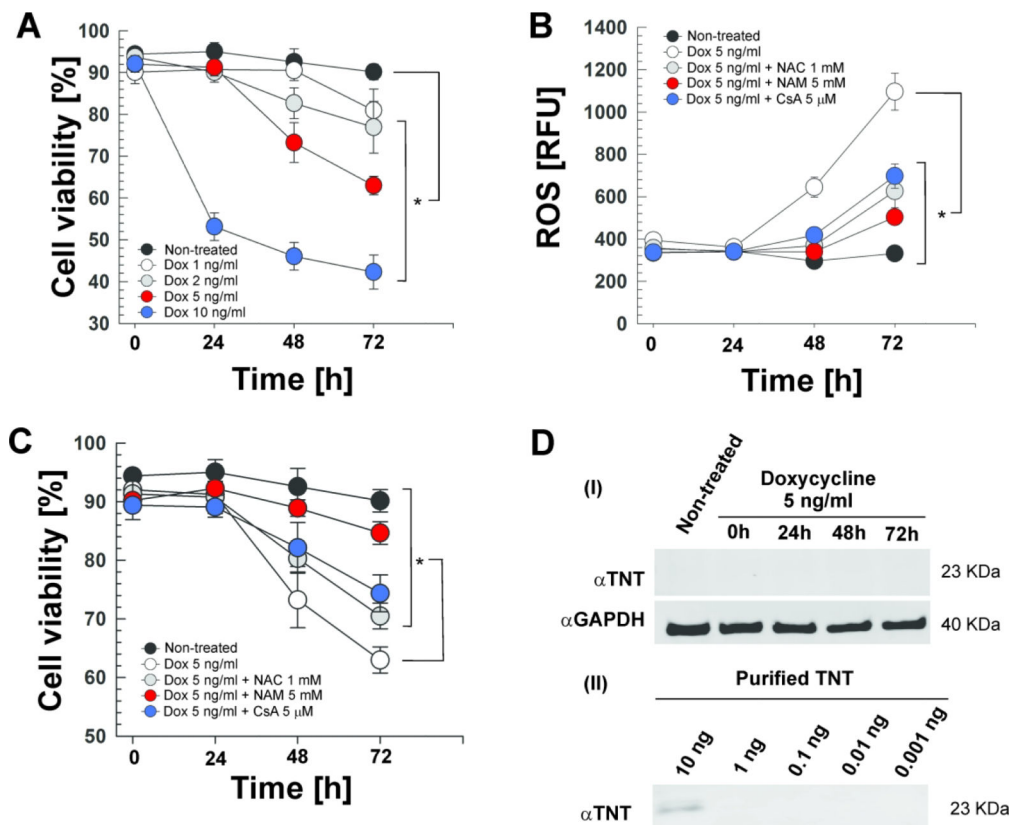
Figure 3. TNT is sufficient to induce lethal oxidative stress in Jurkat-T cells.
Expression of TNT in the Jurkat-T cell line containing an integrated Tet-regulated TNT expression cassette (Jurkat 655-TNT) was induced with different doxycycline (Dox) concentrations at the indicated time points. When indicated, cells were treated with N-acetyl-cysteine (NAC, 1 mM), nicotinamide (NAM, 5 mM) or cyclosporin A (CsA, 5 μM). **(A, C)** Cell viability was measured by trypan blue staining. **(B)** ROS levels were measured with the fluorescent probe H_2DCFDA. **(D)** Western blot for (i) TNT (purified specific polyclonal antibody) and GAPDH (loading control) in the whole-cell lysates of Jurkat 655-TNT cells induced with 5 ng/mL doxycycline at the indicated time points, and for (ii) different amounts of purified WT TNT protein to determine the purified specific αTNT polyclonal antibody sensitivity. Asterisks indicate significant differences at 72 h (p-value<0.01, calculated using the One-way ANOVA with Bonferroni's correction) compared with the indicated conditions. Data are represented as mean ± SEM.
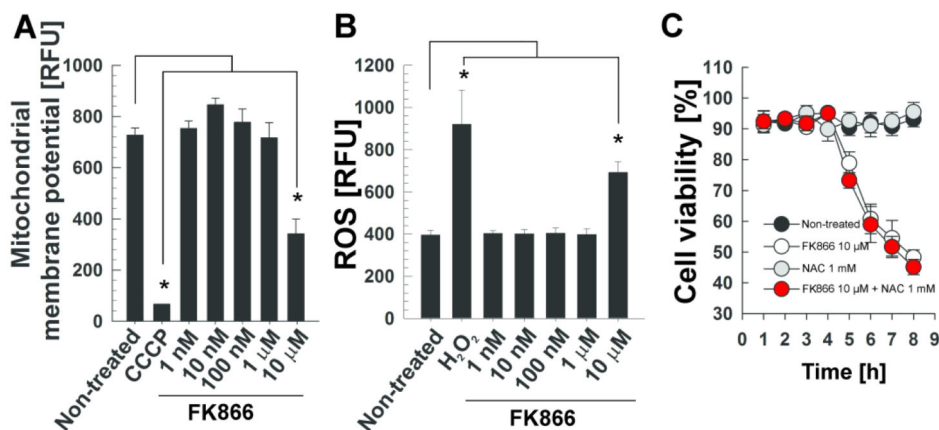
NAD+ depletion induces ROS in macrophages

Figure 4. NAD$^+$ depletion induces ROS in macrophages.
THP-1 macrophages were treated with the indicated concentrations of FK866 for 6 h and
(A) the mitochondrial membrane potential (analyzed by using a JC-1 dye-based fluorescent
probe) and **(B)** ROS levels (measured with the fluorescent probe H$_2$DCFDA) were analyzed.
THP-1 macrophages were treated with CCCP (4 μM) and H$_2$O$_2$ (10 mM, 30 min) as positive
controls for mitochondrial membrane depolarization and ROS detection, respectively. **(C)**
THP-1 macrophages were treated with FK866 at 10 μM and/or N-acetyl-cysteine (NAC) at 1
mM for 6 h, and cell viability was measured by trypan blue. Asterisks indicate significant
differences (p-value<0.01, calculated using the One-way ANOVA with Bonferroni's
correction) compared with the indicated conditions. Data are represented as mean ± SEM.
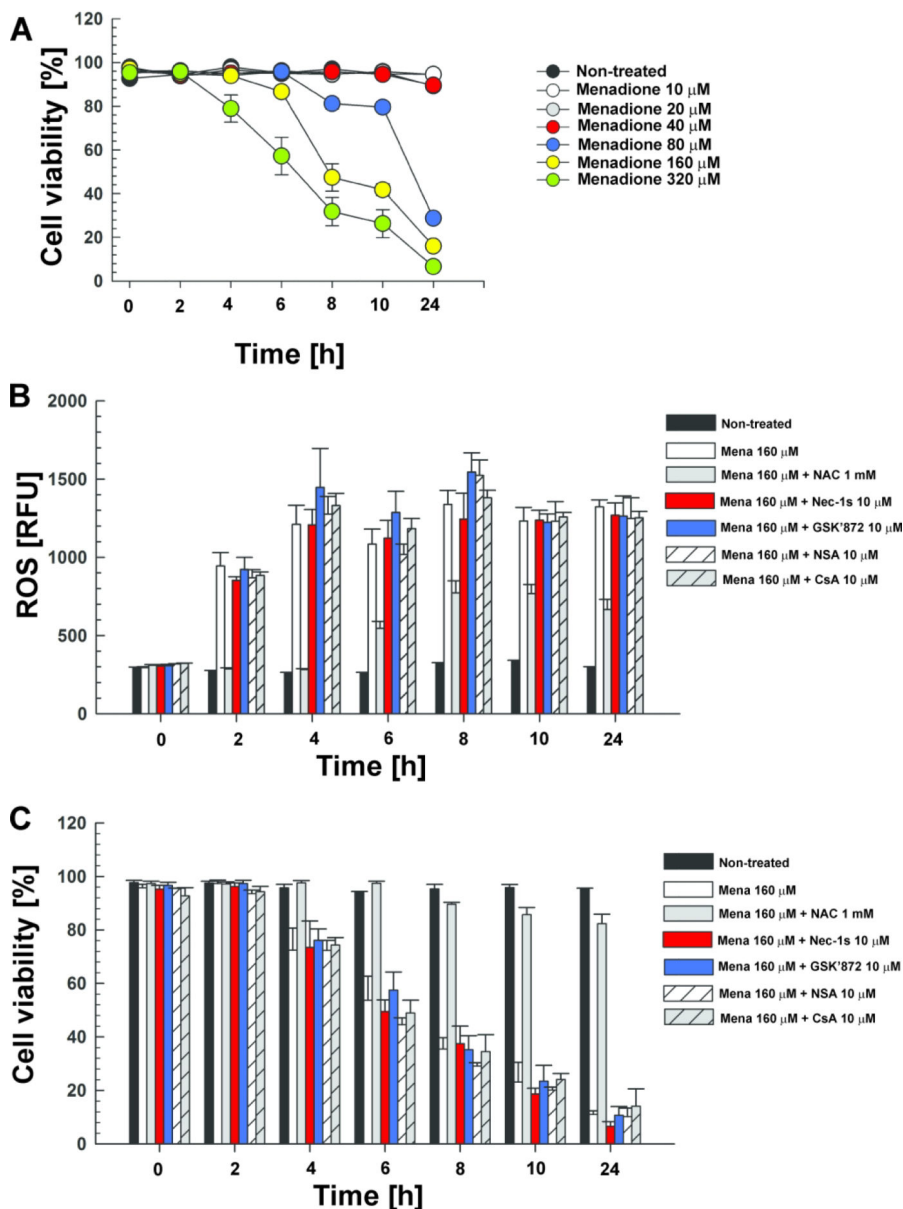
Figure 5. ROS do not activate necroptosis in macrophages.
(A) THP-1 macrophages were treated with different menadione concentrations and cell viability was measured at the indicated time points by trypan blue. THP-1 macrophages were treated with menadione (Mena, 160 μM), N-acetyl-cysteine (NAC, 1 mM), necrostatin-1s (Nec-1s, 10 μM), GSK'872 (10 μM), necrosulfonamide (NSA, 10 μM) and cyclosporin A (CsA, 5 μM), and **(B)** ROS levels (measured with the fluorescent probe H_2DCFDA) and **(C)** cell viability (measured by trypan blue) were determined. Data are represented as mean ± SEM.
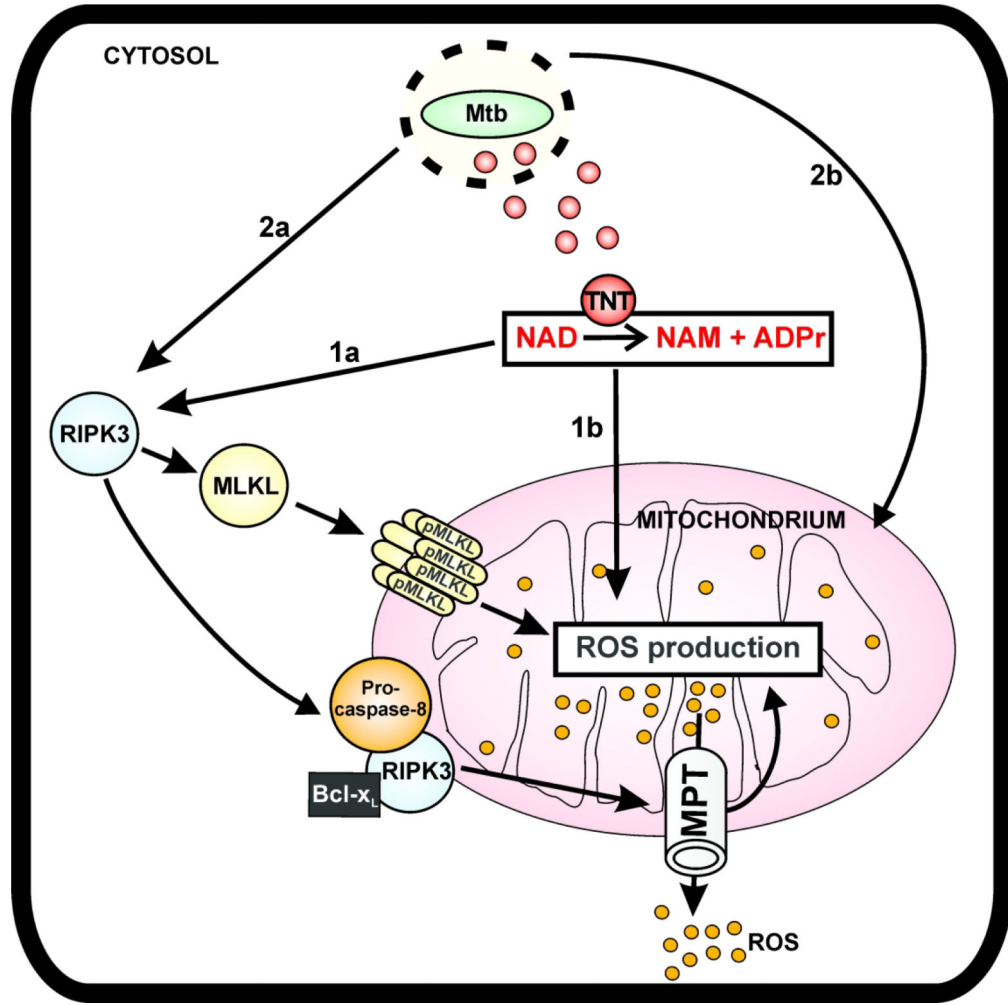
Figure 6. Model of ROS production in macrophages infected with Mtb.
After phagocytosis, Mtb permeabilizes the phagosomal membrane enabling the translocation of TNT to the cytosol (Sun et al., 2015). TNT hydrolyzes the cytosolic NAD^+ to nicotinamide (NAM) and ADP-ribose (ADPr), activating the necroptosis effectors RIPK3 and MLKL (Pajuelo et al., 2018). Activated RIPK3 migrates to the mitochondria and recruits Bcl-x_L (Zhao et al., 2017). The RIPK3-Bcl-x_L complex prevents caspase-8 activation and, together with oligomerized pMLKL, induces ROS production by opening the mitochondrial permeability transition (MPT) pore and other mechanisms (**pathway 1a**). The enzymatic activity of TNT also increases ROS production in a necroptosis-independent manner as a consequence of either NAD^+ depletion or by signaling of the NAD^+ hydrolysis products (**pathway 1b**). Additionally, necroptosis is activated by Mtb in a TNT-independent manner and induces ROS accumulation by the RIPK3/MLKL pathway (**pathway 2a**). Other uncharacterized Mtb factors also contribute to ROS production in macrophages infected with Mtb in a TNT- and necroptosis-independent manner (**pathway 2b**).

Table 1:

Strains and plasmids used in this work.

Strain/Plasmid	Description	Source or reference
Strain		
M. tuberculosis H37Rv	Wild-type	ATCC 25618
M. tuberculosis ML845	H37Rv derivative, unmarked mutant of *cpnT*	(Danilchanka et al., 2014)
M. tuberculosis ML2001	ML845 derivative, L5::pML3009, Kan^R	(Danilchanka et al., 2014)
M. tuberculosis ML2502	ML845 derivative, L5::pML3167, Kan^R	(Pajuelo et al., 2018)
Plasmid		
pML1995	pML1970 derivative, pBR322 origin, bla, lacIq, p$_{T7lac}$-HIS-*malE*-POLYN-TEV-*tnt-rv3902c*, 7677 bp	(Sun et al., 2015)
pML3009	PBR322 origin, aph, L5 attP, FRT-int-P$_{imyc}$-*esxF-esxE-cpnT-rv3902c*-FRT, 9790 bp	(Danilchanka et al., 2014)
pML3167	PBR322 origin, aph, L5 attP, FRT-int-P$_{imyc}$-*esxF-esxE-cpnT$_{H792N/Q822K}$-rv3902c*-FRT, 9789 bp	(Sun et al., 2015)